Economic Geology, v. 107, pp. 1557–1570

Detailed Morphology and Structure of an Active Submarine Arc Caldera: Brothers Volcano, Kermadec Arc*

R. W. Embley,[1,†] C. E. J. de Ronde,[2] S. G. Merle,[3] B. Davy,[2] and F. Caratori Tontini[2]

[1] *Pacific Marine Environmental Laboratory, National Oceanic and Atmospheric Administration, 2115 SE O.S.U. Dr., Newport, Oregon 97365-5258*

[2] *GNS Science, PO Box 30-368, Lower Hutt 5040, New Zealand*

[3] *Cooperative Institute for Marine Resources Studies, Oregon State University, 2115 SE O.S.U. Dr., Newport, Oregon 97365-5258*

Abstract

A survey of the Brothers caldera volcano (Kermadec arc) with the autonomous underwater vehicle *ABE* has revealed new details of the morphology and structure of this submarine frontal arc caldera and the geologic setting of its hydrothermal activity. Brothers volcano has formed between major SW-NE–trending faults within the extensional field of the Havre Trough. Brothers may be unique among known submarine calderas in that it has four active hydrothermal systems, two high-temperature sulfide-depositing sites associated with faulting on the northwestern and western walls (i.e., the NW caldera and W caldera hydrothermal sites, respectively), and gas-rich sites on the summits of the constructional cones that fill most of the southern part of the caldera (i.e., the Upper and Lower cone sites). The 3.0- × 3.4-km caldera is well defined by a topographic rim encompassing ~320° of its circumference and which lies between the bounds of two outer half-graben–shaped faults in the northwest and southeast sectors. There is not a morphologically well defined continuous ring fault (at the map resolution), although near-vertical scarps are present discontinuously at the base of sections of the wall. The width of the wall varies from <200 m at its southwest portion to ~750 m on its northern section. The widest part of the wall is its northwest sector, which also has the largest documented area of hydrothermal alteration and where sea-floor magnetization is lowest. In addition to primary northwest-southeast elongation and southwest-northeast structures caused by faulting within the regional back-arc strain field, there are also less well developed west-southwest–north-northeast regional structures intersecting the volcano that is apparent on the *ABE* bathymetry and at outcrop scale from submersible observations. Asymmetrical trap-door–style caldera collapse is considered a possible mechanism for the formation of the Brothers caldera.

Introduction

Fossil submarine calderas are common sites of mineralization in the continental record due to the presence of fracture-controlled hydrothermal circulation fueled by multiple cycles of magmatic activity (Stix et al., 2003; Franklin et al., 2005). Submarine calderas are common on volcanoes along modern intraoceanic arcs (de Ronde et al., 2003a, 2007; Wright et al., 2006). They occur in a wide range of water depths with variable magma chemistry and their submarine mineralization processes have been of increasing interest because of the high amount of magmatic gases common in the arc setting that appear to enhance the concentrations of Au and Cu especially (e.g., de Ronde et al., 2011). In recent years these sites have become exploration targets for sea-floor mining companies (Hoagland et al., 2010). Characterization of the detailed morphology and structure of modern submarine arc calderas has only recently begun with the acquisition of high-resolution multibeam bathymetric surveys in these settings (Wright et al., 2006; de Ronde et al. 2007; Embley et al., 2008). However, even the best ship-borne multibeam systems have limited resolution in the water depths of many calderas (>1,000 m) where the complex morphology of the steep caldera walls is particularly difficult to image.

In order to improve our understanding of the submarine arc caldera and its mineralization processes we wanted to survey a hydrothermally active arc caldera with the highest resolution near-bottom multibeam system along with sensors to measure hydrothermal signals in the water column and the magnetic field. In June 2007, we used the autonomous underwater vehicle *ABE* (Autonomous Benthic Explorer) to conduct a series of dives focused on mapping the well-studied Brothers caldera in the southern Kermadec arc (Figs. 1–3).

Brothers volcano is a relatively young, ~7- × 11-km volcanic edifice centered at 34°52.5′ E, 179°4.0′ S along the southern Kermadec frontal magmatic arc (Fig. 1). This volcanic edifice has a quasirectangular base approximately enclosed by the 2,000-m contour with its long axis oriented NW-SE (Figs. 1, 2). The regional bathymetry suggests that Brothers may have begun to form by eruptions within a graben structure between the regional faults (noted as RTRs in Fig. 1) that bound the present extent of the volcano. The slight NW-SE elongation of the Brothers volcano is approximately parallel to the regional extension direction of ~N 130°–140° E as defined by Campbell et al. (2007), indicating that regional tectonic stresses have influenced the evolution of the volcano. A 3.0- × 3.4-km summit caldera with up to 300 m of relief and maximum depth of 1,879 m encloses two cones, the southern Upper cone rising to 1,196 m and the Lower cone to its northeast shoaling to 1,304 m.

Brothers volcano has been the focus of an expanding series of studies beginning in the 1990s when it was first mapped and its hydrothermal systems discovered and initially characterized (Wright et al., 1998; Wright and Gamble, 1999; de Ronde et al., 2001, 2003b). Brothers is currently the most active site for hydrothermal activity along the Kermadec arc and

† Corresponding author: e-mail, robert.w.embley@noaa.gov

* Pacific Marine Environmental Laboratory contribution 3849.

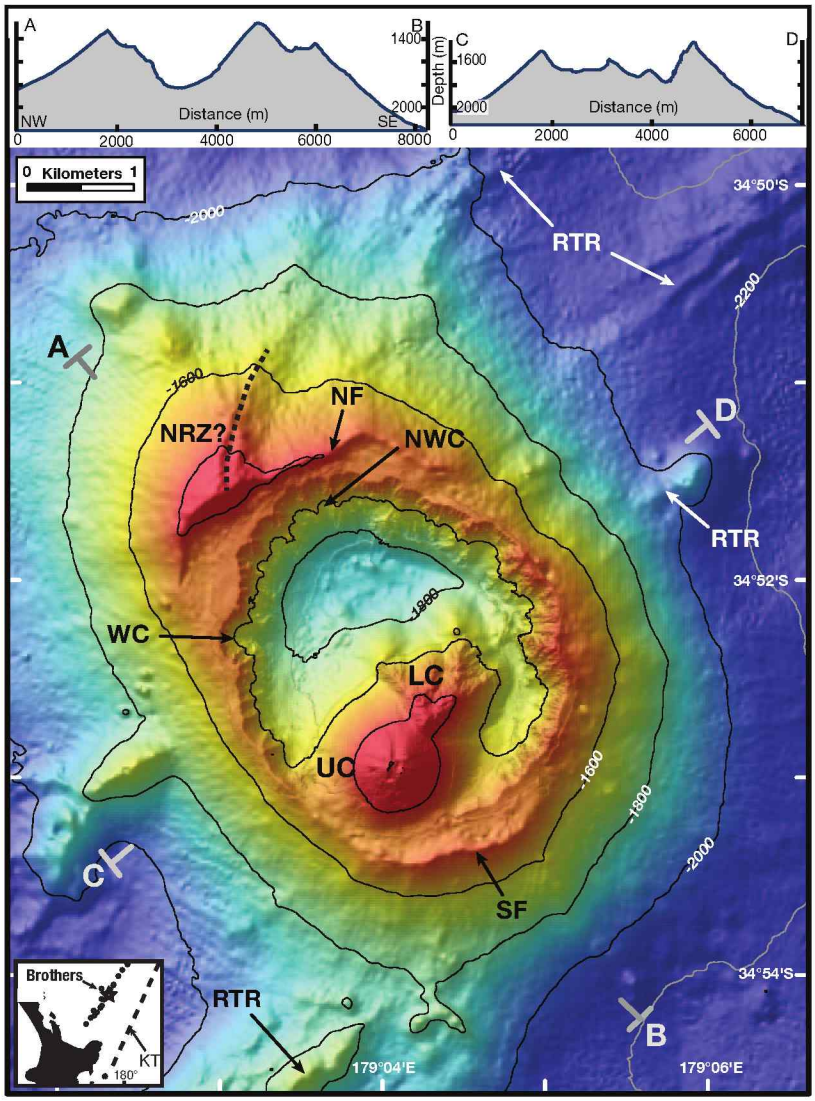

Fig. 1. Detailed bathymetry of Brothers volcano and its environs. Dashed lines are structural ridges. Letters designate North fault (NF), South fault (SF), North rift zone (NRZ), South rift zone (SRZ), Upper cone (UC), and Lower cone (LC), NW caldera (NWC), W caldera (WC), and regional tectonic ridge (RTR). Letters A-B, C-D are endpoints for the bathymetric cross sections shown in the top panel. Contour interval is 200 m. Inset: KT = Kermadec Trench.

has been the most intensely studied of any of the Kermadec volcanoes surveyed to date (de Ronde et al., 2005, 2011). There are three active hydrothermal sites previously described in some detail both from the water column plumes (de Ronde et al., 2005) and by in situ observations and sampling (de Ronde et al., 2011). The NW caldera wall hydrothermal site (Figs. 1, 4) includes an area of at least 500 × 500 m over a depth range between 1,692 and 1,543 m characterized by high-temperature venting from sulfide edifices and an outer zone characterized by low-temperature venting, altered rock and sediment, and inactive hydrothermal deposits (de Ronde et al., 2005, 2011). Both of the cones have hydrothermal systems at their summit. The Lower cone has an intense discharge of diffuse fluids over most of its summit area. The Upper cone has several sites of diffuse discharge on and near its summit and at least one higher temperature vent with more focused discharge. Vents from both of the cones contain magmatic volatiles that produce low pH fluids relative to the higher temperature hydrothermal fluids venting from the NW caldera wall site (de Ronde et al., 2005). A fourth active site was found on the west wall (herein named the W caldera wall site; "WC," Fig. 1) during the *ABE* survey with the water column sensor package (Baker et al., 2012) and high-temperature venting was found here on a subsequent dive using the *Kiel 6000* remotely operated vehicle (ROV). Finally, dredged sulfides from the SE caldera and/or wall indicate the presence of an extinct hydrothermal system (de Ronde et al., 2005). Some water column anomalies were detected over this site that could indicate some continued diffuse venting (Baker et al., 2012).

Our main objective was to obtain colocated, near-bottom, high-resolution data sets including bathymetry and total magnetic field to map areas of hydrothermal alteration—and measurements from several oceanographic sensors to map

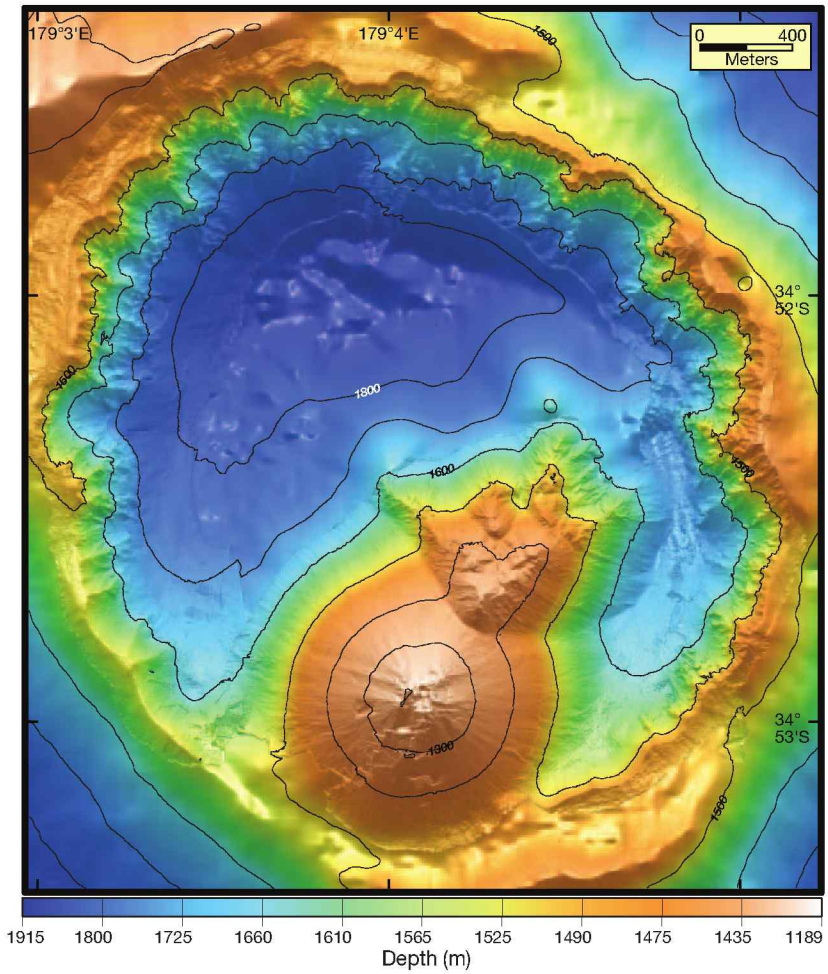

FIG. 2. High-resolution (~2 m grid) mapping of the caldera walls and cones from *ABE*, combined with EM300 bathymetric surveys (~25-m resolution) data for the caldera floor and upper flanks of the caldera. *ABE* dive tracks shown in Figure 3A. Contour interval is 100 m.

the presence and character of hydrothermal effluent rising from the seafloor of the entire caldera, in order to construct a detailed picture of the volcano structure and distribution of hydrothermal activity. The morphology of the Brothers caldera using the new 2-m grid of the caldera wall, rim, and intracaldera cones is described and interpreted in detail in this paper. A detailed description of the magnetic data and inversion methodology is presented and discussed here in the context of the caldera structure by Caratori Tontini et al. (2012). Water column results derived from *ABE* are presented in Baker et al. (2012). Additional papers on Brothers by Berkenbosch et al. (2012), Ditchburn et al. (2012), and Gruen et al. (2012) also draw on some of the results presented here.

Methods

Research vessel operations

The ROVARK (remotely operated vehicle ARK [for Arc]) expedition of July 2007 was a collaborative effort between NOAA (United States), GNS Science (New Zealand), IFM-GEOMAR (Germany), and Woods Hole Oceanographic Institute (United States), using the R/V *Sonne*. In addition to the *ABE* dives on Brothers volcano several dives of the new remotely operated vehicle (ROV) *Kiel 6000* were conducted at targets of interest identified during the *ABE* dives. There were also regional mapping surveys with a hull-mounted EM120 multibeam sonar system and water column surveys (not discussed here).

ABE surveys and data

The *ABE* was a fully autonomous underwater vehicle operated by Woods Hole Oceanographic Institute for more than 15 years (Yoerger et al., 2007a, b). Standard instrumentation on the vehicle used during the 2007 ROVARK expedition were (1) a SIMRAD SM2000, 200-kHz multibeam sonar, (2) a three-component Develpco fluxgate magnetometer, (3) a SeaBird 9/11+ CTD system, (4) a SeaPoint optical backscatter sensor, and (5) an ORP (oxidation-reduction potential) sensor developed by K. Nakamura of AIST (Japan; Baker et al., 2012).

ABE was navigated by a combination of long baseline acoustic navigation system using four bottom-moored transponders and a bottom-lock acoustic doppler unit that measured speed over bottom between acoustic fixes (Yoerger et al., 2007a, b). The vehicle completed 140 h of survey time in seven successful dives (204-210) of which 96 h were in bottom survey

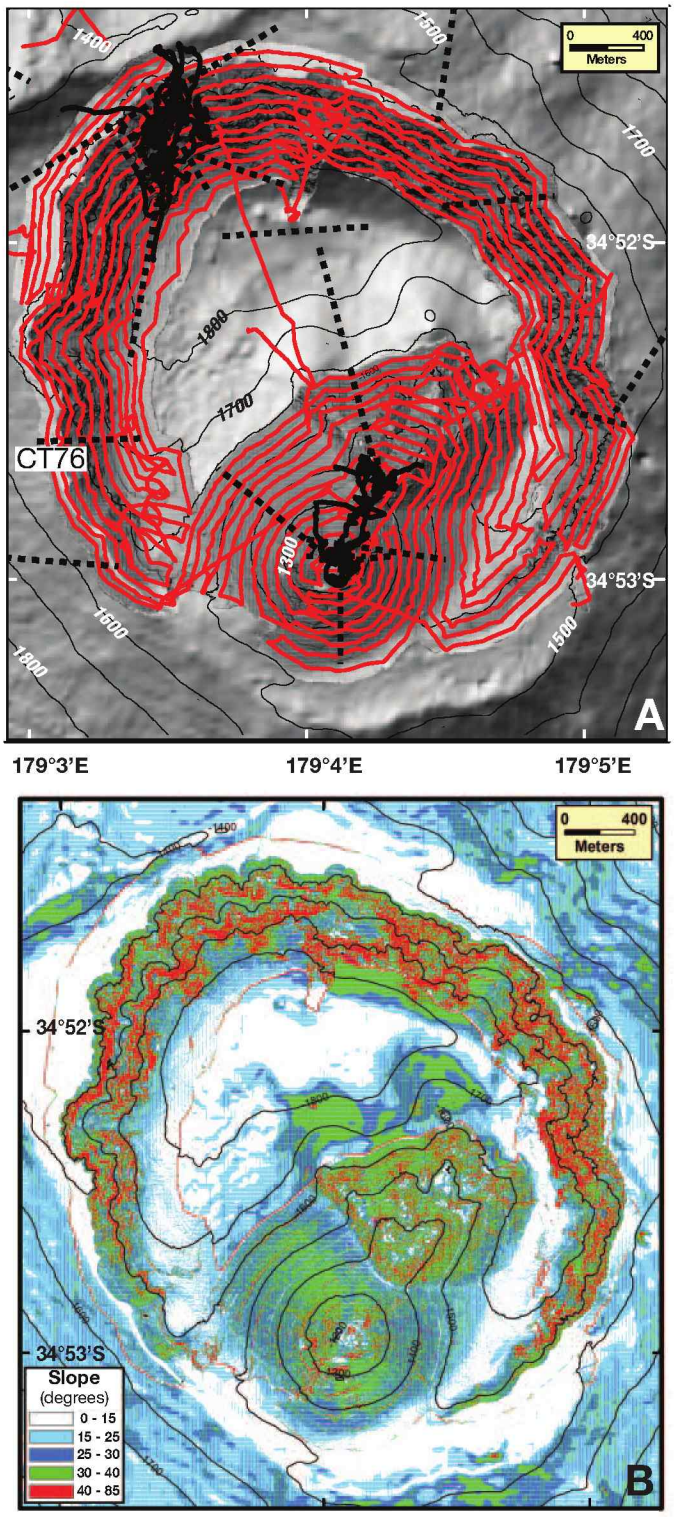

FIG. 3. A. Dive and tow tracks: Red = *ABE* AUV tracks; solid black lines = *Shinkai 6500* and *Pisces V* submersible dive tracks; black dashed lines = camera tows taken from the R/V *Tangaroa* in 2010 (Clark et al., 2010). Contours (gray lines) are at 100-m intervals. B. Sea-floor slope derived from bathymetric grid using the ArcMap© slope function. Five slope intervals are used for simplification (see legend). Contours (gray lines) are at 100-m intervals.

mode, with the remainder accounted for by descent, ascent, and wait-time for the R/V *Sonne* to return to the area (Fig. 3A). A total of 161 km of survey was completed during the mission. The *ABE* tracks were laid out in arcs parallel to the contours due to the steep caldera walls, typically ~50 m apart at an altitude of 52 ± 8 m above the seafloor. Significant portions of two dives were designed to measure hydrothermal flux from the NW caldera and cone sites (Baker et al., 2012). There was insufficient time to complete the *ABE* survey of the caldera floor or to extend the survey out from the caldera rim toward the older summit structure to the northwest. The final *ABE* bathymetry data were gridded at 2 m (grid cell size), which is the resolution used for the maps in this study. Slope values were calculated using ArcMap© (Fig. 3B). Geologic interpretations of structures and volcanic features were made on the basis of these grids (Fig. 4).

Submersible dives

Nine submersible dives were made in the Brothers caldera (Fig. 3A) prior to the 2007 expedition. Four *Shinkai 6500* dives were conducted in November 2004 and provided reconnaissance information of the NW caldera wall hydrothermal system (851 and 852) and the constructional cones in the south 853 and 854; see de Ronde et al., 2011). The *Shinkai 6500* dive program was followed in 2005 with a dive program using the *Pisces V* submersible. Four of the dives targeted the NW caldera wall site (626, 628, 631, and 632) and one on the cones (630; also see de Ronde et al., 2011, fig. 2). Video tapes of all the dives at Brothers were reviewed and notations of geologic and hydrothermal features were entered into a spreadsheet and plotted as overlays on the *ABE* bathymetry in the ArcMap© program.

Morphology of the Brothers Summit and Caldera

Brothers summit

The shallowest point of Brothers, at 1,196 m, is the summit of the Upper cone in the southwest quadrant of the caldera. Outside the caldera, the summit of Brothers is broadly defined by two rectilinear ridges (RTRs in Fig. 1) bounding its northwest and southeast sides (Figs. 1, 2), which we will refer to as the North and South faults. The North fault (NF) has a throw of 150 m and forms the southern edge of a high area (shallowest point ~1,305 m indented by what we interpret to be a low-relief rift zone extending north-northeast (~N 005° E) from its summit. The steeper southeastern side of the North fault implies it is a southeast-facing fault (half-graben?) oriented at N 062° E, approximately the orientation of the regional tectonic ridges described earlier that intersect the northern part of the volcano. The South fault (SF), in contrast to its northern counterpart, is lower in relief (40 m) and is steepest on its outer convex side. It overlaps the topographic rim of the caldera in the east and merges with it on its western side. Its longer middle section is oriented slightly more easterly (~N 072° E) than its northern counterpart. These two bounding structures are not obviously linked topographically.

Caldera nomenclature

In this paper, we use the terminology of Lipman (1997) to describe the morphology of volcanic calderas as shown in

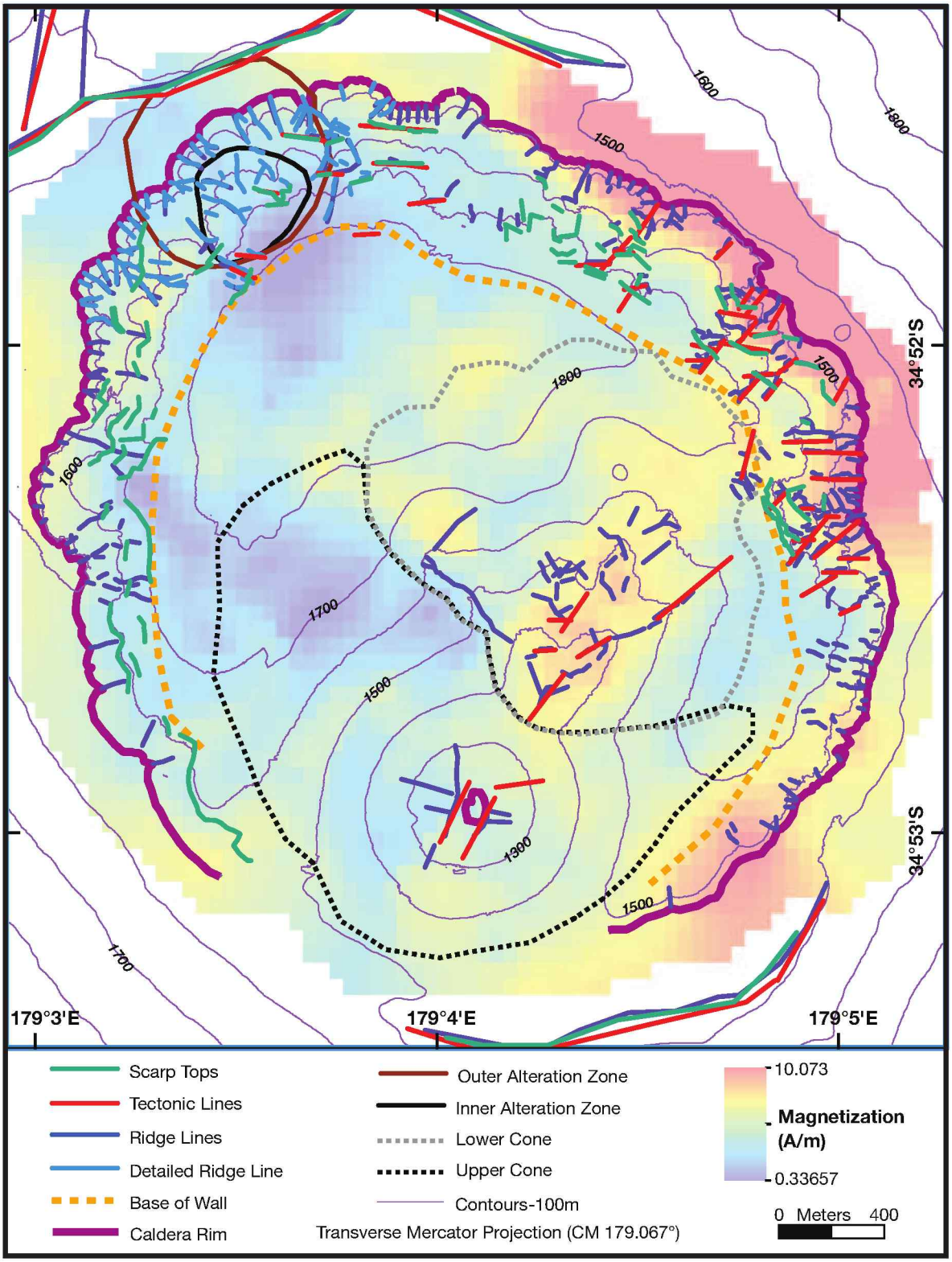

FIG. 4. Geologic classification of caldera underlain by magnetization. Contours (purple lines) are at 100-m intervals. Magnetization of caldera from *ABE* survey (also see Caratori Tontini et al., 2012). Units are amperes/meter (A/m). Black circular outline ("Inner alteration zone") on northwest caldera wall shows extent of active venting and intense alteration defined by submersible dives. Larger brown circular line ("Outer alteration zone) indicates area of alteration and venting defined by additional data from de Ronde et al. (2005, 2011) and Baker et al. (2012).

Figure 5A. Although this scheme was developed for subaerial volcanoes, we believe that the basic mechanical process applies equally to submarine calderas. It should be noted, however, that Lipman's classification is for larger volcanic systems, with a minimal size of about 4 to 5 km of topographic diameter (cf. Brothers at ~3.5 km). Also, we use the term "caldera fill" instead of "dominant tuff fill" because submarine caldera fill (particularly in the deep water of the Brothers caldera) is likely deposited by gravity flows rather than pyroclastic flows.

This generalized model for caldera formation assumes a piston-type collapse from a sudden deflation of a magma chamber (Fig. 5A-C). Modeling of caldera formation using inflated balloons in sandboxes has shown that the primary piston collapse induces two types of faulting (e.g., Acocella et al., 2000, Roche et al., 2000; Holohan et al., 2005; Acocella, 2007; Howard, 2010); a near-vertical, or outward dipping primary fracture (or ring fault), and penecontemporaneous inward-dipping normal faults forming outside the initial piston collapse. The former defines the structural limit of the caldera and the outermost faulting of the latter type defines the caldera's topographic boundary. The dip of the primary ring fault in extensional settings was shown by Holohan (2005) to be almost vertical (Fig. 5B, C). Secondary sliding of high-angle blocks is also common in the modeling studies (Roche et al., 2000; Fig. 5D).

Caldera rim

The topographic rim of the caldera can be traced for about 320° of the summit of the volcano; it is not clearly defined in the southern sector where the Upper cone merges with the older summit region (Figs. 1, 2, 6). The diameter of this topographic Brothers caldera is ~3.0 × 3.4 km. The rim depth only varies by about 100 m around the caldera, from a minimum of ~1,420 m in the NE quadrant (near the 8,000 m marker) to a maximum of ~1,520 in the SE quadrant (from the 0 to the 1,400-m markers; Fig. 6). The most uniform depth of the rim occurs on the northwest and northern sections where it occurs around ~1,470 ± 15 m.

Caldera subsidence fracture system

As discussed above, calderas formed by piston-like subsidence have a structural ring fault system (Lipman, 1997) marking the initial piston collapse (Fig. 5A). However, there is not a continuous well-defined base-of-the-wall ring fracture system in the Brothers caldera, although there are steep, nearly vertical, laterally discontinuous scarps of 20 m or greater relief that could be structures associated with the primary collapse of the caldera (Figs. 4, 7, 8). The discontinuous trace of this ring fault marked by near-vertical scarps (shown by arrows in the profiles in Fig. 7) is probably partially buried as a consequence of mass wasting events derived from the upper wall. The tops of the most prominent of these scarps range from about 1,560 to 1,710 m (a shallow exception at ~1,500-m depth in the 2,000-m marker profile is within a major secondary slide scar). The lack of a continuous structure, particularly in the region of the northwest wall, could be in part due to hydrothermal alteration whereby the rock is too weak to form a prominent scarp and burial is by material mass wasted from the walls. Using the deepest scarps as a guide, we estimate the structural caldera size to be 2.2 to 2.6 km in diameter.

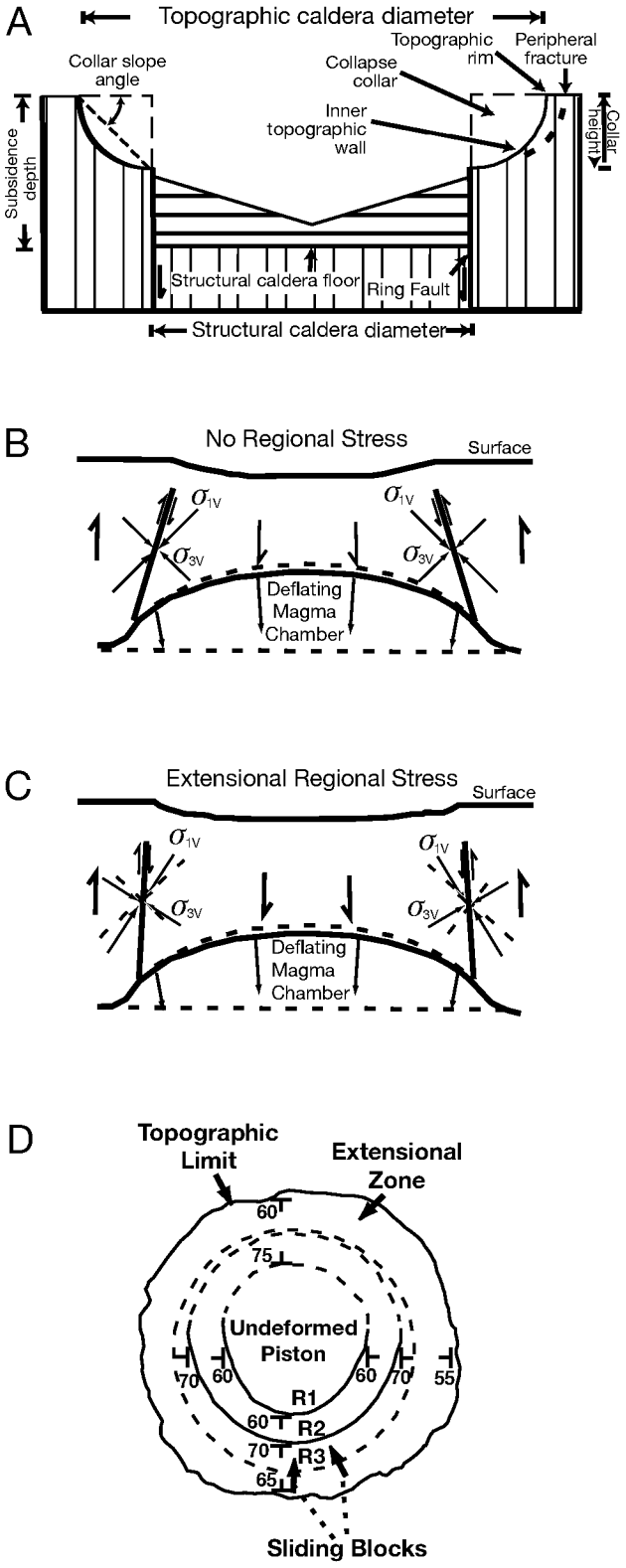

FIG. 5. Caldera structure and modeling. A. Cross section of idealized caldera showing structural features, after Lipman (1997). B. Two-dimensional view of stresses and fault orientations for caldera prior to formation with no regional stress (modified after Holohan et al., 2005, fig. 6). C. Same as (B) but with extensional regional stress (modified after Holohan et al., 2005, fig. 6). D. Plan view of sketch of caldera formed in sandbox model (modified after Roche et al., 2000, fig. 13).

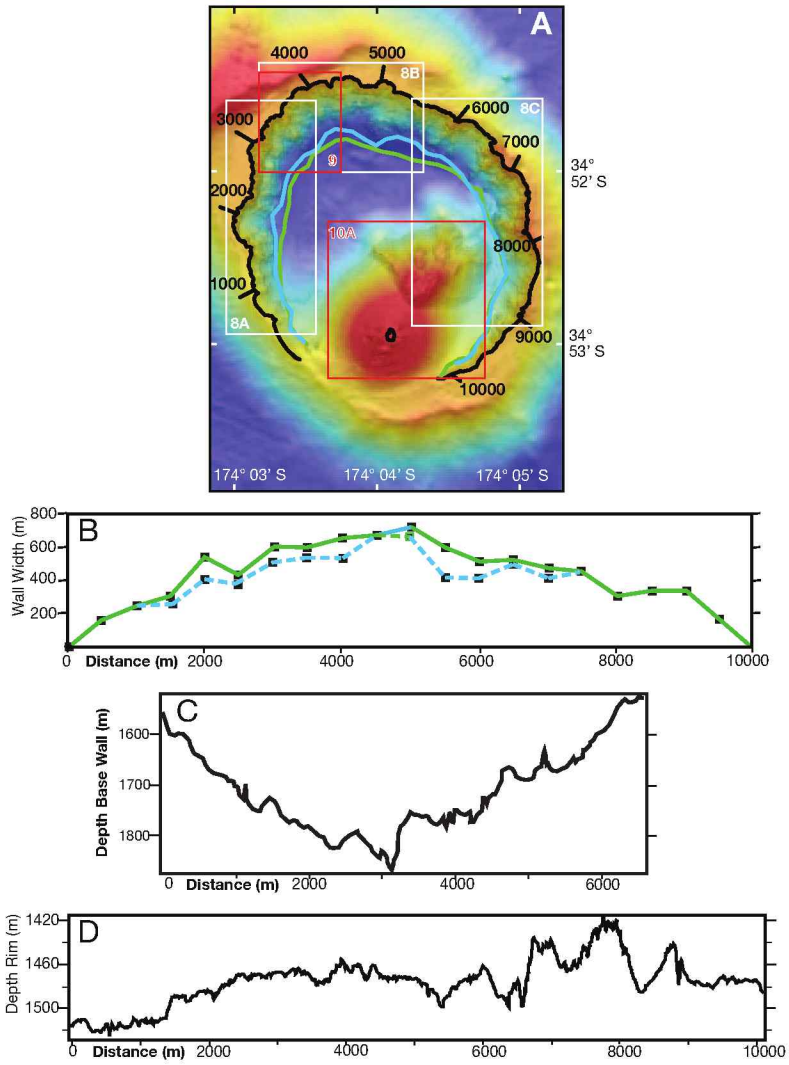

FIG. 6. A. Map of caldera showing distances in meters along caldera rim which serves as reference point for (B), (C), and (D) and for the bathymetric cross sections shown in Figure 7. The blue line is base of wall estimated by extrapolating between locations of deepest outcrops and green line is estimate of base of wall using the break in slope. Boxes locate more detailed maps in Figures 8 and 9A. B. Plot of distances from caldera rim to base of wall (width of wall). Blue and green lines use matching base of wall estimates in Figure 9A. C. Plot of depth of base of wall. D. Plot of depth of rim of caldera.

Inner topographic caldera wall

Lipman (1997) defined the inner topographic caldera wall as the area between the topographic rim and the primary fracture system along which the caldera subsided. We have roughly defined its lower bound by interpolating between the deepest outcrops which we think define the remnant of the ring fault. Its lower bound also roughly marks a transition to an aggraded slope at about 25° (Figs. 3B, 7). This angle was chosen because the angle of repose is 27° to 35° (depending on material properties) on submarine volcaniclastic slopes (Lee et al., 1994; Sansone and Smith, 2006).

We classify outcrops as having slopes >40°—a conservative number, and a slightly higher value than the angle of response, in order to account for material that could be cemented by hydrothermal precipitates. Using this value, outcrops comprise at least a third of the total wall area (Figs. 3B, 4). The remaining area is fine- to coarse-grained material and heavily eroded altered outcrops. The pattern of erosion and outcrops also varies along the wall (Figs. 2, 7, 8). For example, the outcrops on the west-northwest and north sections of the caldera wall are mostly benches of limited lateral continuity (Fig. 7). The most extensive outcrops are on the northeast and east wall sections which coincide approximately with the shallowest sections of the rim. Relatively scarp free portions of the caldera wall occur in the extreme southeast and southwest sectors of the volcano, in close proximity to the intra-caldera cone complex. These sections also have less relief (~200 m) and do not have a well-developed secondary drainage pattern compared to other parts of the wall (Figs. 2, 8). This suggests that these sections never had as much relief as other sections of the caldera wall. Conversely, the cone building proximal to these sections may have diminished the original relief in these areas by deposition of fine-grained volcaniclastics during postcaldera eruptive episodes.

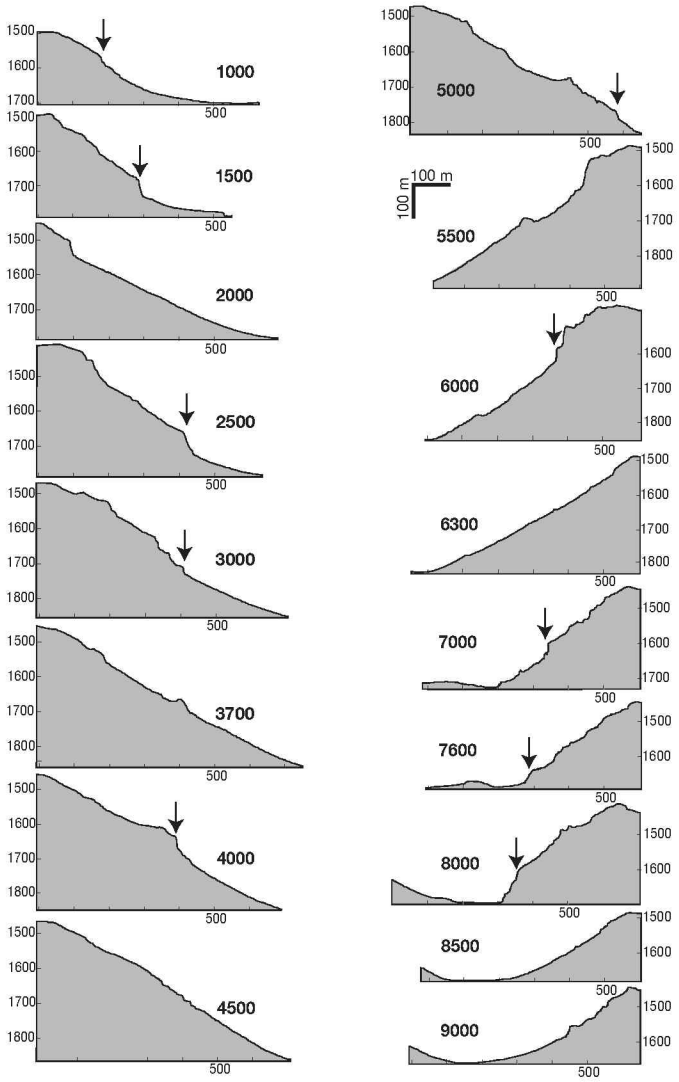

FIG. 7. Bathymetric cross sections of the Brothers caldera wall (numbers are meters along rim in clockwise direction; see Fig. 6A). Arrows show location of the steepest scarps.

The relief of the caldera wall varies from less than 100 m on the southwest and southeast terminations, to 400 m on the northwest end of the caldera. The wall relief is variable, depending on the area of rock outcrops. Some of the deeper, discontinuous steep scarps probably mark the trace of the main caldera ring fault (Fig. 7). The width of the wall, here defined as the horizontal distance between the deepest wall remnants and the topographic rim, is widest at the northwest end (~600 m) and narrows to ~200 m on the southwest and southeast terminations.

The wide northwest wall of the Brothers caldera (i.e., location of the NW caldera wall hydrothermal site; Figs. 8B, 9) has the most robust and extensive hydrothermal activity in the caldera. The hydrothermal deposits have been studied in detail by de Ronde et al. (2003b, 2005, 2011) and Berkenbosch et al. (2012) and will not be discussed in detail here. The hydrothermal deposits and alteration zones of the northwest wall cover a wide area of at least 500 × 500 m. (Figs. 1, 4). At least some of the active, high-temperature sites appear to line up on fracture systems oriented ~N 290° E surrounded by extinct chimneys, diffuse venting, nontronite chimneys, and intensely altered (from high-temperature fluids) rock and volcaniclastic deposits. The pervasive, high-temperature (up to 302°C; de Ronde et al., 2005, 2011) hydrothermal fluids passing through the rocks and forming the mineral deposits here have altered some of the lavas to predominantly low-density clays such as have been described on the Galapagos Ridge (Embley et al., 1988). This intense alteration is considered more extensive at depth and is the presumptive origin of the broad low magnetization anomaly that is centered over this part of the volcano (Fig. 4; also see Caratori Tontini et al., 2012).

Although there are no systematic submersible surveys of the rest of the caldera wall, water column measurements made by *ABE* discovered high-temperature venting on the west wall (Baker at al., 2012) followed by a test dive using the *Kiel 6000* ROV during the 2007 ROVARK cruise that discovered high-temperature venting in a canyon here (W caldera wall site). A camera tow made in 2010 (Tangaroa 2010 Station 76, Fig. 3A) just south of the large indentation in the W caldera wall site shows apparent extensive altered rocks and oxide deposits infiltrating the seafloor, consistent with hydrothermal activity in this area. Finally, a dredge made in the SE caldera during the 1998 R/V *Sonne* cruise recovered some sulfides and/or altered rocks from the lower slopes of the caldera wall (Wright et al., 1998; de Ronde et al., 2005).

Cones and caldera floor

Constructional volcanism fills most of the southern half of the caldera (Figs. 1, 2). The topographic summit of Brothers volcano (1,196 m) is the top of the Upper cone (Fig. 10A, B). This feature is a symmetrical, largely undissected constructional cone that fills the southwest sector of the caldera. Most of the flanks of the Upper cone have a slope of about 27° to 32°, which, as stated above, is within the range of the angle of repose for volcaniclastic material. Locally, steeper slopes (Fig. 3B) occur mostly on the summit area and on the upper flanks in a few places where there have been recent slumps.

The summit of the Upper cone (Fig. 10B) consists of a pair of SW-NE–trending ridges that are roughly parallel to the regional tectonic trend that bound a series of nested, semienclosed, 10- to 20-m-deep depressions that are likely remnants of formerly active pit craters. The youngest volcanic feature on the summit of the Upper cone is probably the fully enclosed, 40-m diam, 20-m deep crater located at its northern end (Fig. 10B). There were no fresh-appearing volcaniclastic deposits and/or lava flows observed on the summit. The uppermost flank of the cone is in a state of degradation; several recent slumps on the northeast and southeast flanks have exposed some thick columnar jointed lava flows (Fig. 10B).

The summit area of the Upper cone has patchy venting over a zone about 250 m in diameter. Numerous sulfur deposits occur in the form of surface veneers from water column fallout, crusts, chimneys, and flows (noted in Fig. 10B). Diffuse venting dominates this area (i.e., 46°–68°C) with focused venting much less apparent. The hottest temperature recorded was 122°C at a small "white smoker" on the northwest rim of the 20-m-deep, 40-m-diameter crater (de Ronde

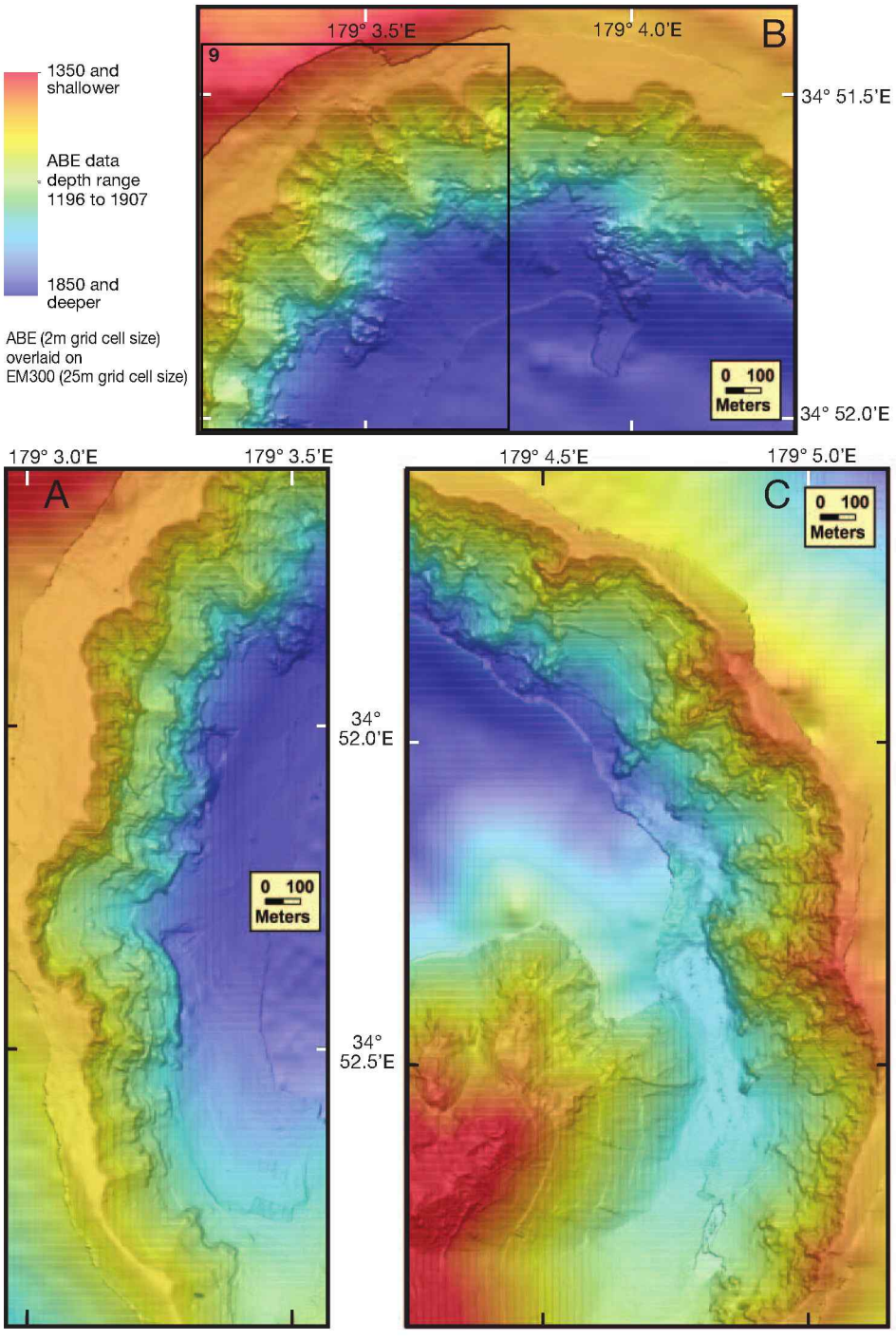

FIG. 8. Close-up maps of select sections of the caldera walls at Brothers using *ABE* 2-m grid (locations given by boxes in Fig. 6). A. West and southwest sectors of the caldera. B. Northwest and north sectors (location of intense hydrothermal activity). Box shows location of Figure 9. C. East and southeast sectors.

et al., 2011). Large mounds of sulfur were observed and sampled in, and around, the crater while sulfur flows are found within ~20 m to the north and south (Fig. 10B, de Ronde et al., 2011) signifying that this crater has most likely contained liquid sulfur in the recent past, which has occasionally extruded onto the seafloor. Tall (up to 6 m) sulfur chimneys were also found inside the main pit crater (Fig. 10B, de Ronde et al., 2011). It is not clear when the last volcanic eruption of the Upper cone occurred. Fresh volcaniclastic deposits and/or lava flows were not observed on its summit and the uppermost flank of the cone is in a state of degradation—several recent slumps on the northeast and southeast flanks have exposed some thick columnar jointed lava flows (Fig. 10B).

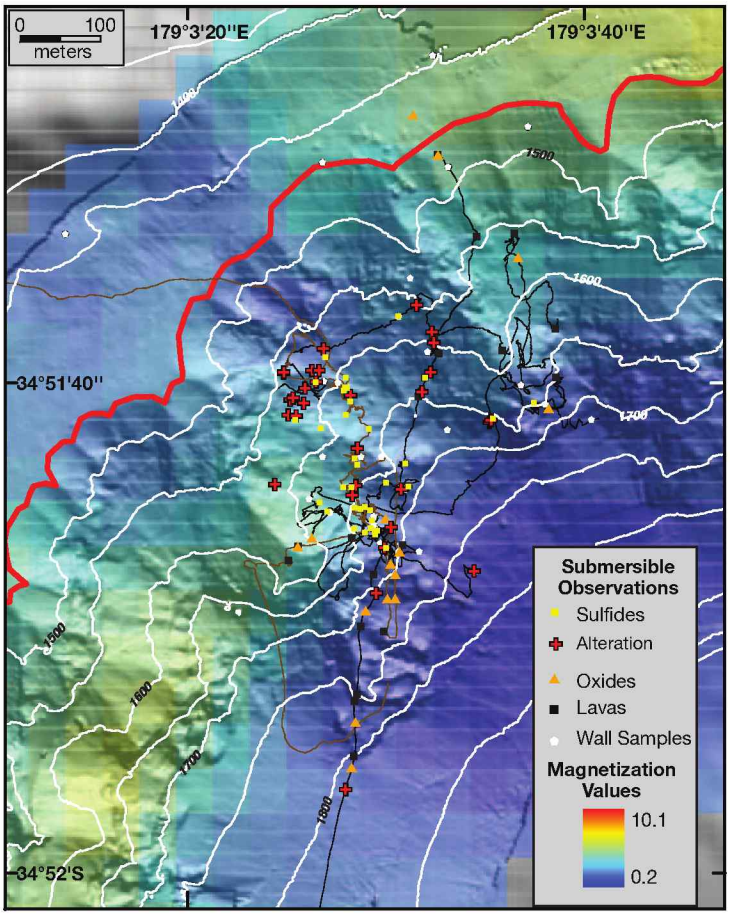

FIG. 9. Detailed bathymetry of the hydrothermal area on NW caldera wall hydrothermal zone. Hill shade image of topography is overlain by semitransparent layer of crustal magnetization (also see caption for Fig. 4). Contours are at 50 m on the *ABE* bathymetry grid. Location of area shown in Figures 6A and 8B.

The Upper cone onlaps the Lower cone, an older more deeply dissected terrane that extends northeast from the Upper cone's northeast base. (cf. de Ronde et al., 2011; Figs. 2, 10A, C). Mass wasting has removed portions of the Lower cone's north and northwest flanks, leaving a series of gullied ridges extending to the north and northwest. The most prominent of these ridge strikes perpendicular to, and directly northwest from, the summit of the Lower cone. Several other ridges radiate from the summit to the north and northeast. Locally, steep slopes occur on the walls of these gullies where outcrops have been observed by camera tows (Clark et al., 2010) and submersible dives. By comparison, the eastern flank of the Lower cone is relatively undissected.

The summit of the Lower cone lies along a SW-NE trend from the crest of the Upper cone. The summit of the Lower cone (Fig. 10C) is a triangular-shaped area with a narrow ridge oriented NNE and several smaller ridges radiating away from it and does not have any first-order volcanic features, such as pit craters. Its irregular morphology is consistent with shaping by degradational processes. The steepest slopes on the summit area are on the east side of the summit ridge where there appears to have been a recent slump (off a fault?), exposing thick columnar-jointed lava flows. However, even on the gullied northwest flank of the Lower cone, the slopes do not typically exceed 40° as they do in many places on the caldera wall (Fig. 3B). The valleys between the ridges are finer grained volcaniclastic material. The summit of the Lower cone is characterized by sulfur crusts, pervasive diffuse venting of up to 68°C (Fig. 10C, de Ronde et al., 2011) from about the 1,235-m contour to the summit ("white dashed line," Fig. 10C) making an active area of ~150 m in diameter (Fig. 9C, de Ronde et al., 2011). Extensive colonies of long-necked barnacles, swarms of shrimp, zoarcid fish, crabs, and patches of bacterial mat are found on the summit region and along the eastern summit scarp (Fig. 10C, de Ronde et al., 2011).

Most of the northwest portion of the caldera floor (Fig. 2) was not surveyed by *ABE* because of time constraints so the map resolution is much lower than the rest of the caldera (i.e., 25 m from shipborne multibeam versus 2 m for the *ABE* bathymetry). Much of this area is hummocky terrane that is probably slump material from the walls or the cones. A ridge and swale pattern highlighted on the slope map (Fig. 3B) on the lowermost northwest flank of the Upper cone appear to be low relief sediment waves probably formed by downslope sediment flow.

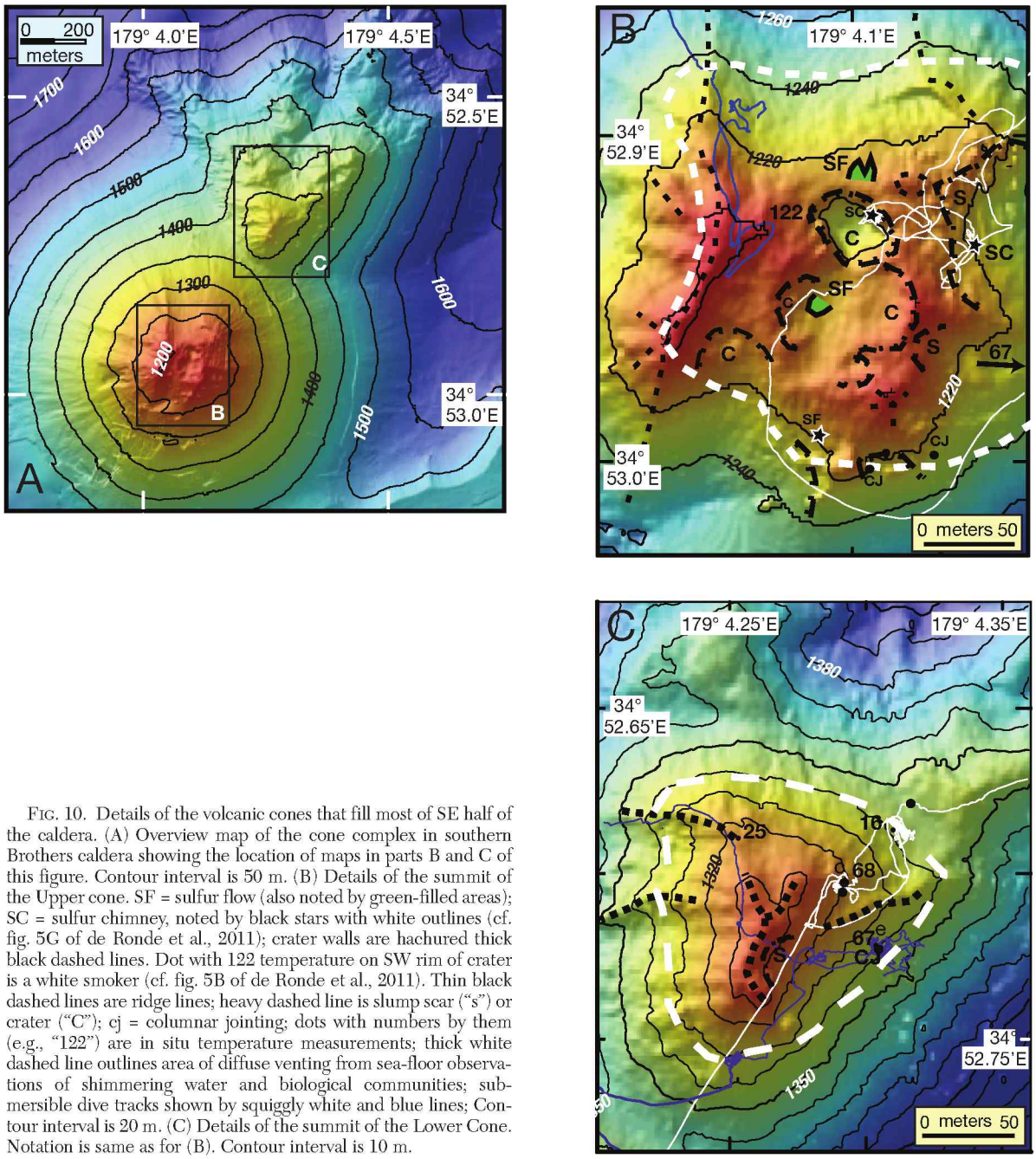

FIG. 10. Details of the volcanic cones that fill most of SE half of the caldera. (A) Overview map of the cone complex in southern Brothers caldera showing the location of maps in parts B and C of this figure. Contour interval is 50 m. (B) Details of the summit of the Upper cone. SF = sulfur flow (also noted by green-filled areas); SC = sulfur chimney, noted by black stars with white outlines (cf. fig. 5G of de Ronde et al., 2011); crater walls are hachured thick black dashed lines. Dot with 122 temperature on SW rim of crater is a white smoker (cf. fig. 5B of de Ronde et al., 2011). Thin black dashed lines are ridge lines; heavy dashed line is slump scar ("s") or crater ("C"); cj = columnar jointing; dots with numbers by them (e.g., "122") are in situ temperature measurements; thick white dashed line outlines area of diffuse venting from sea-floor observations of shimmering water and biological communities; submersible dive tracks shown by squiggly white and blue lines; Contour interval is 20 m. (C) Details of the summit of the Lower Cone. Notation is same as for (B). Contour interval is 10 m.

Structures

It is difficult to identify subtle tectonic overprinting fractures on a circular caldera wall because the caldera-forming process and subsequent mass wasting produces fractures both parallel and perpendicular to the rim. However, careful examination of topographic "hillshade" grids from different "sun" angles shows that there does appear to be a consistent well-defined E-W or slightly NW-SE fabric that is independent of the local wall orientation (Figs. 2, 4, 8). This fabric is most prominent in the north, northeast, and eastern sectors of the wall. There is also somewhat less convincing complementary southwest-northeast fabric (i.e., parallel to the regional fabric) that is most evident in the northeast and east sectors. Sea-floor observations made from submersibles indicate that the east-west fracture system is present at outcrop scale at least in the mineralized area on the northwest wall (see below). Unfortunately, the submersible observations cover only a small percentage of the entire caldera wall.

Discussion and Conclusions

The high-resolution *ABE* multibeam bathymetry presents a more detailed view of the Brothers caldera. Although this enhanced map does not clearly define surface faulting, we can infer some aspects based on the existing morphologic data

and underlying magnetic signature of the volcano, when compared to recent results of caldera formation modeling. For example, sandbox modeling studies of caldera formation have shown that faulting directly associated with magma withdrawal and/or eruption from the underlying magma chamber produces a piston collapse characterized by either vertical faults, or slightly outward-dipping faults, forming primary deep-seated faults with secondary inward-dipping normal faults on the outside (Marti et al., 1994; Roche et al., 2000; Holohan et al., 2005; Howard, 2010). These secondary, inward-dipping normal faults probably are the main conduits for present-day hydrothermal activity, with some ~east-west and other cross fracturing. For a caldera formed in an extensional regime such as Brothers, it is likely that the normal faults would best develop perpendicular to the regional extension direction, in this case along southwest-northeast trends. The half-graben structures bounding the south-southwest and northwest summit of Brothers could represent an initial stage of this process. Intersection of the normal fault zones with the primary ring faults could result in enhanced circulation of seawater as recharge to the hydrothermal system (cf. Gruen et al., 2012), while continued regional extension would tend to keep the fracture system open to hydrothermal circulation over an extended period of time (cf. ages of 1,200 years for the oldest mineralization at Brothers; de Ronde et al., 2011; Ditchburn et al., 2012).

The Brothers caldera measures 3.0 × 3.4 km using the topographic rim. Assuming that there was a piston-type collapse and using the base of the wall as defined by interpolating the deepest steep discontinuous scarps assumed to trace the main caldera ring fault the structural caldera measures 2.2 × 2.6 km, considerably smaller than those normally associated with such collapses on terrestrial volcanoes (Lipman, 1997). The widest portion of the wall coincides with the large hydrothermal system located on the northwestern wall, which probably is largely due to persistent slope degradation as a consequence of long-term, high-temperature hydrothermal alteration underlying this area. Although a portion of the ellipticity of the topographic caldera is from this enhanced hydrothermal alteration of the NW caldera wall site (hence making the wall wider there), the outline of the structural caldera as determined by the morphology is still slightly elliptical with its major axis in the NW-SE orientation.

The high-resolution bathymetric survey results presented here do not clearly delineate a continuous ring fracture. Wright and Gamble (1999) postulated that the Brothers caldera probably formed incrementally because of the apparent lack of a continuous ring fracture system. However, neither is there any clear pattern of multiple phases of caldera formation as would likely be evidenced by semicontinuous major vertical benches on the wall. The lack of a defined through-going ring fracture on the southern part of the caldera might be due to burial by postcaldera volcaniclastic deposition from the cones. However, it is also possible that the Brothers caldera formed asymmetrically as a "trapdoor" caldera with the northwest quadrant being downfaulted along a hinge line on the southeast portion. In this interpretation, the ring fault might not propagate all the way around to the south, or would have a smaller throw in that section. The northwest portion of the ring fault would continue to be a weak zone created from persistent long-term extension of the Havre Trough. This hypothesis is consistent with the long-term, high-temperature hydrothermal system and pervasive alteration zone on the NW caldera wall site.

The most recent volcanic activity in the Brothers caldera has been the Upper cone rising from the southernmost caldera; the new, high-resolution bathymetry clearly shows it lapping the Lower cone and reveals well-defined pit craters on its summit. Very young sulfur deposits and vents showing a clear magmatic degassing component is present on its summit (de Ronde et al., 2011) and shallow seismicity and harmonic tremor have been recorded from beneath this region of the caldera (Dziak et al., 2008). The age of the last volcanic event on the Upper cone is not known. However, recent observations of active submarine arc volcanoes (Embley et al., 2006; Chadwick et al., 2008, 2012; Wright et al., 2008) have shown that aggradational and degradational processes on their summits can be directly related to recent eruptions and can significantly alter the morphology of the summit and flank over short periods of time. By contrast, the older Lower cone, lapped by the northern flank of the Upper cone, is heavily dissected on its north side. The summit of the Lower cone does not retain any primary volcanic features, although it has extensive diffuse venting centered about the summit area. However, it is still host to hydrothermal activity but of arguably slightly less magmatic influence (de Ronde et al., 2011).

The cones appear to be lined up approximately along the orientation of regional structures and there are also low-relief structures to the southwest and northeast of the caldera that are similarly oriented (Figs. 1, 2). We propose that the onset of volcanic activity began along an underlying southwest-northeast fracture, possibly the hinge line on the southeast part of the caldera following major caldera formation. The eruption of the Lower cone sequence might have begun as a fissure eruption and evolved to a point source (Upper cone) in the mode of Hawaiian fissure eruptions (Bruce and Huppert, 1989). It is likely that both were constructed after the caldera formed, although the deep erosion of the north and northwest slopes of the Lower cone could have been triggered by some vertical motion of the caldera.

Brothers volcano provides us with insight into a large range of active hydrothermal processes affecting a submarine arc volcano. It is one of the few sites where there is both a high-temperature sulfide system and a magmatically driven degassing system within a young caldera. It is important to note, however, that we lack information that is critical to making definitive interpretations about the evolution and deep structure of Brothers. In particular, there is scant information on volcanic stratigraphy (including the fate of the material that was ejected from, or injected into, dikes as the caldera formed), geochronology, structural mapping at an outcrop scale (except at small areas on the summits of the cones and the NW caldera wall hydrothermal zones), long-term local seismicity, and detailed subsurface structural information. In any case, it is likely that Brothers and a few other active arc volcanoes will be our first choice laboratories for studying arc-related hydrothermal systems for some time to come.

Acknowledgments

First and foremost we are grateful to the *ABE* group for their skill and dedication in obtaining the high-quality data set during the expedition. We also thank Colin Devey and Geomar for their collaboration on board the R/V Sonne, the shipboard complement, and the science team for excellent support at sea. I.C. Wright, D.J. Fornari, and M.I. Leybourne provided helpful reviews of the paper and W.W. Chadwick provided valuable advice on the references. Funding was generously provided by the NOAA Office of Ocean Exploration, the NOAA Vents program and GNS Science, New Zealand. PMEL contribution no. 3849.

REFERENCES

Acocella, V., 2007, Understanding caldera structure and development: An overview of analogue models compared to natural calderas: Earth-Science Reviews, v. 85, p. 125–160.

Acocella, V., Cifelli, F., and Funiciello, R., 2000, Analogue models of collapse calderas and resurgent domes: Journal of Volcanology and Geothermal Research, v. 104, p. 81–96.

Baker, E.T., Walker, S.L., Embley, R.W., and de Ronde, C.E.J., 2012, High-resolution hydrothermal mapping of the Brothers caldera, Kermadec arc: Economic Geology, v. 107, p. 1583–1593.

Berkenbosch, H.A., de Ronde, C.E.J., Gemmell, J.B., McNeill, A.W., and Goemann, K., 2012, Mineralogy and formation of black smoker chimneys from the Brothers submarine volcano, Kermadec arc: Economic Geology, v. 107, p. 1613–1633.

Bruce, P.M., and Huppert, H.E.,1989, Thermal control of basaltic fissure eruptions: Nature, v. 342, p. 665–667.

Campbell, M.E., Rowland, J.V., Wright, I.C., and Smith, I.E.M., 2007, Oblique rifting along the central and southern Kermadec arc front (30°–36°S), SW Pacific: Geochemistry, Geophysics, Geosystems, v. 8, doi:10.1029/2006GC001504.

Caratori Tontini, F., Davy, B., de Ronde, C.E.J., Embley, R.W., Leybourne, M., and Tivey, M.A., 2012, Crustal magnetization and the hydrothermal system at Brothers volcano, southern Kermadec arc, New Zealand: Economic Geology, v. 107, p. 1571–1581.

Chadwick, W.W., Jr., Wright, I.C., Schwarz-Schampera, U., Hyvernaud, O., Reymond, D., and de Ronde, C.E.J., 2008, Cyclic eruptions and sector collapses at Monowai submarine volcano, Kermadec arc: 1998–2007: Geochemistry, Geophysics, Geosystems, v. 9, doi:10.1029/2008GC002113.

Chadwick, W.W., Jr., Dziak, R.P., Haxel, J.H., Embley, R.W. and Matsumoto, H., 2012, Submarine landslide triggered by volcanic eruption recorded by in-situ hydrophone: Geology, v. 40, p. 51–54, doi:10.1130/G32495.1.

Clark, C., Consalvey, M., Baird, S., Schnabel, K., Stewart, R., Mitchell, J., Hart, A., Herrera, S., Beaumont, J., Hill, P., Schwarz, J., and Holman, M., 2010, Voyage report of seamounts on the southern Kermadec arc (TAN1007): Second leg, biology, project report: DSKB103, June, 2010, 48 p.

de Ronde, C.E.J., Baker, E.T., Massoth, G.J., Lupton, J.E., Wright, I.C., Feely, R.A., and Greene, R.R., 2001, Intra-oceanic subduction-related hydrothermal venting, Kemadec volcanic arc: Earth and Planetary Science Letters, v. 193, p. 359–369.

de Ronde, C.E.J., Massoth, G.J., Baker, E.T., and Lupton, J.E., 2003a, Submarine hydrothermal venting related to volcanic arcs: Society of Economic Geologists Special Publication 10, p. 91–109.

de Ronde, C.E.J., Faure, K., Bray, C.J., Chappell, D.A., and Wright, I.C., 2003b, Hydrothermal fluids associated with seafloor mineralization at two southern Kermadec arc volcanoes, offshore New Zealand: Mineralium Deposita, v. 38, p. 217–233.

de Ronde, C.E.J., Hannington, M.D., Stoffers, P., Wright, I.C., Ditchburn, R.G., Reyes, A.G., Baker, E.T., Massoth, G.J., Lupton, J.E., Walker, S.L., Greene, R.R., Soong, C.W.R., Ishibashi, J., Lebon, G.T., Bray, C. J., and Resing, J. A., 2005, Evolution of a submarine magmatic-hydrothermal system: Brothers volcano, southern Kermadec arc, New Zealand: Economic Geology, v. 100, p. 1097–1133.

de Ronde, C.E J., Baker, E.T., Massoth, G.J., Lupton, J.E., Wright, I.C., Sparks, R.J., Bannister, S.C., Reyners, M.E., Walker, S.L., Greene, R.R., Ishibashi, J., Faure, K., Resing, J.A., and Lebon, G.T., 2007, Submarine hydrothermal activity along the mid-Kermadec arc, New Zealand: Large-scale effects on venting: Geochemistry, Geophysics, Geosystems, v. 8, Q07007.

de Ronde, C.E.J., Massoth, G.J., Butterfield, D.A., Christenson, B.W., Ishibashi, J., Ditchburn, R.G., Hannington, M.D., Brathwaite, R.L., Lupton, J.E., Kamenetsky, V.S., Graham, I.J., Zellmer, G.F., Dziak, R.P., Embley, R.W., Dekov, V.M., Munnik, F., Lahr, J., Evans, L.J. & Takai, K., 2011, Submarine hydrothermal activity and gold-rich mineralization at Brothers volcano, Kermadec arc, New Zealand: Mineralium Deposita, v. 46, p. 541–584, DOI 10.1007/s00126-011-0345-8.

Ditchburn, R.G., de Ronde, C.E.J., and Barry, B.J., 2012, Radiometric dating of volcanogenic massive sulfides and iron oxide crusts with an emphasis on $^{226}Ra/Ba$ and $^{228}Ra/^{226}Ra$ in volcanic and hydrothermal processes at intraoceanic arcs: Economic Geology, v. 107, p. 1635–1648.

Dziak, R.P., Haxel, J.H., Matsumoto, H., Lau, T.K., Merle, S.G., de Ronde, C.E.J., Embley, R.W., and Mellinger, D.K., 2008, Observations of regional seismicity and local harmonic tremor at Brothers volcano, south Kermadec arc, using an ocean bottom hydrophone array: Journal of Geophysical Research-Solid Earth, v. 113, doi:10.1029/2007JB005533.

Embley, R.W., Jonasson, I.R., Perfit, M.R., Franklin, J.M., Tivey, M.A., Malahoff, A., Smith, M.F., and Francis, T.J.G., 1988, Submersible investigation of an extinct hydrothermal system on the Galapagos Ridge: Sulfide mounds, stockwork zone, and differentiated lavas: Canadian Mineralogist, v. 26, p. 517–539.

Embley, R.W., Chadwick, W.W., Jr., Baker, E.T., Butterfield, D.A., Resing, J.A., de Ronde, C.E.J., Tunnicliffe, V., Lupton, J.E., Juniper, S.K., Rubin, K.H., Stern, R.J., Lebon, G.T., Nakamura, K., Merle, S.G., Hein, J.R., Wiens, A., and Tamura, Y., 2006, Long-term eruptive activity at a submarine arc volcano: Nature, v. 441, p. 494– 497, doi:10.1038/nature04762.

Embley, R.W., de Ronde, C.E.J., and Ishibashi, J., 2008, Introduction to special section on active magmatic, tectonic and hydrothermal processes at intraoceanic arc submarine volcanoes: Journal of Geophysical Research–Solid Earth, v. 113, doi:10.1029/2008JB005871.

Franklin, J.M., Gibson, H.L., Jonasson, I.R., and Galley, A.G., 2005, Volcanogenic massive sulfide deposits: Economic Geology 100th Anniversary Volume, p. 523–560.

Gruen, G., Weis, P., Driesner, T., de Ronde, C.E.J., and Heinrich, C.A., 2012, Fluid-flow patterns at Brothers volcano, southern Kermadec arc: Insights from geologically constrained numerical simulations: Economic Geology, v. 107, p. 1595–1611.

Hoagland, P.S. Beaulieu, S., Tivey, M., Eggert, R., German, C., Glowka, L., and Lin, J., 2010, Deep-sea mining of seafloor massive sulfides: Marine Policy, v. 34, p. 728–732.

Holohan, E.P., Troll, V.R., Walter, T.R., Munn, S., McDonnell, S., and Shipton, Z.K., 2005, Elliptical calderas in active tectonic settings: An experimental approach: Journal of Volcanology and Geothermal Research-Solid Earth, v. 144, p. 119–136.

Howard, K.A., 2010, Caldera collapse: Perspective from comparing Galapagos volcanoes, nuclear-test sinks, sandbox models and volcanoes on Mars: GSA Today, v. 20, no. 10, p. 4-10, doi: 10.1130/GSATG82A.1.

Lee, H.J., Torres, M.E., and McArthur, W., 1994, Stability of submerged slopes on the flanks of the Hawaiian islands, a simplified approach: U.S. Geological Survey Open-File Report, 94-638, 54p.

Lipman, P.W., 1997, Subsidence of ash-flow calderas: Relation to caldera size and magma-chamber geometry: Bulletin of Volcanology, v. 59, p. 198–218.

Marti, J.A., Ablay, G.J., Redshaw, L.T., and Sparks, R.S., 1994, Experimental studies of collapse calderas: Journal of the Geological Society [London], v. 151, p. 919–929.

Roche, O., Druitt, T.H., and Merle, O., 2000, Experimental study of caldera formation: Journal of Geophysical Research-Solid Earth, v. 105, p. 395–416.

Sansone, F.J., and Smith, J.R., 2006, Rapid mass wasting following nearshore submarine volcanism on Kilauea Volcano, Hawaii: Journal of Volcanology and Geothermal Research, v. 151, p. 133–159.

Stix, J., Kennedy, B., Hannington, M., Gibson, H., Fiske, R., Mueller, W., and Franklin, J., 2003, Caldera-forming processes and the origin of submarine volcanogenic massive sulfide deposits: Geology, v. 31, p. 375–378.

Wright, I.C., and Gamble, J.A., 1999, Southern Kermadec submarine caldera arc volcanoes (SW Pacific): Caldera formation by effusive and pyroclastic eruption: Marine Geology, v. 161, p. 207–227.

Wright, I.C., de Ronde, C.E.J., Faure, K., and Gamble, J.A., 1998, Discovery of hydrothermal sulfide mineralization from southern Kermadec arc volcanoes (SW Pacific), 1998: Earth and Planetary Science Letters, v. 164, p. 335–343.

Wright, I.C., Worthington, T. J., and Gamble, J.A., 2006, New multibeam mapping and geochemistry of the 30°-35° S sector, and overview, of southern Kermadec arc volcanism: Journal of Volcanology and Geothermal Research, v. 149, p. 263–296.

Wright, I.C., Chadwick, W.W., Jr., de Ronde, C.E.J., Reymond, D., Hyvernaud, O., Gennerich, H.-H., Stoffers, P., Mackay, K., Dunkin, M., and Bannister, S.C., 2008, Collapse and reconstruction of Monowai submarine volcano, Kermadec arc, 1998–2004: Journal of Geophysical Research-Solid Earth, v. 113, doi: 10.1029/2007JB005138.

Yoerger, D.R., Jakuba, M., Bradley, A.M., and Bingham, B., 2007a, Techniques for deep sea near-bottom survey using an autonomous underwater vehicle: International Journal of Robotics Research, v. 26, p. 41–54, doi:10.1177/0278364907073773.

Yoerger, D.R., Bradley, A.M., Jakuba, M., Tivey, M.A., German, C.R., Shank, T.M., and Embley, R.W., 2007b, Mid-ocean ridge exploration with an autonomous underwater vehicle: Oceanography, v. 20, p. 53–59.